STEM CELLS AND DEVELOPMENT
Volume 23, Number 1, 2014

DOI: 10.1089/scd.2013.0202

Expansion of Hepatic Stem Cell Compartment Boosts Liver Regeneration

Veronika Papp,[1] András Rókusz,[1] Katalin Dezső,[1] Edina Bugyik,[1] Vanessza Szabó,[1] Zoltán Pávai,[2] Sándor Paku,[1,3] and Péter Nagy[1]

The hepatic stem cells reside periportally forming the canals of Hering in normal liver. They can be identified by their unique immunophenotype in rat. The oval cells, the progenies of stem cells invade deep the liver parenchyma after activation and differentiate into focally arranged small—and eventually trabecularly ordered regular hepatocytes. We have observed that upon the completion of intense oval cell reactions narrow ductular structures are present in the parenchyma, we propose to call them parenchymal ductules. These parenchymal ductules have the same immunophenotype [cytokeratin (CK)7 − /CK19 + /alpha-fetoprotein (AFP) − /delta-like protein (DLK) −] as the resting stem cells of the canals of Hering, but different from them reside scattered in the parenchyma. In our present experiments, we have investigated in an *in vivo* functional assay if the presence of these parenchymal ductules has any impact on a progenitor cell driven regeneration process. Parenchymal ductules were induced either by an established model of oval cell induction consisting of the administration of necrogenic dose of carbontetrachloride to 2-acetaminofluorene pretreated rats (AAF/CCl_4) or a large necrogenic dose of diethylnitrosamine (DEN). The oval cells expanded faster and the foci evolved earlier after repeated injury in the livers with preexistent parenchymal ductules. When the animals were left to survive for one more year increased liver tumor formation was observed exclusively in the DEN treated rats. Thus, repeated oval cell reactions are not necessarily carcinogenic. We conclude that the expansion of hepatic stem cell compartment conceptually can be used to facilitate liver regeneration without an increased risk of tumorigenesis.

Introduction

It is well documented in humans, as well as in experimental animals that the stem cell compartment can restore the liver parenchyma after extensive damage [1]. Unfortunately this process is often not efficient enough. The presence of intense ductular reaction in the liver of patients who die of fulminant hepatic failure indicates the activation of the stem cells but obviously they are not able to restore appropriate liver function [2]. The acceleration of the stem cell fed regeneration would have important implications in clinical medicine. We have been analyzing the 2-acetaminofluorene/partial hepatectomy (AAF/Ph) model [3] of liver regeneration for several years [4,5]. In this widely used experimental model the AAF inhibits the regenerative activity of the hepatocytes and the liver mass is restored by the participation of so called oval cells [6]. The oval cells form elongated tubules, which are the extensions of canals of Hering [4]. Later, the oval cells at the distal tip of these tubules gain higher proliferative activity, while differentiating along the hepatocytic lineage. During this process the clusters of small differentiating hepatocytes form foci [7]. This is a relatively synchronized process with well-defined stages of regeneration and differentiation. We have observed scattered ductules (called parenchymal ductules further on) inside the liver lobules 3 months after the completion of this experiment [5], when otherwise the normal histological structure of the liver was restored. Interestingly, the cells constructing these ductules express CK19 but do not CK7, alike the immunophenotype of the normal canals of Hering, which are strictly confined to the periportal space in rat [5]. The AAF/Ph experiment also serves as promoter in the classical Solt-Farber chemical hepatocarcinogenesis model [8], when it is preceded by a single dose administration of diethylnitrosamine (DEN). We have recently demonstrated that the architecture of oval cell proliferation and focus formation is identical whether DEN was or was not given to the rats [7]. However, while analyzing these experiments, we had the impression that the oval cell proliferation/differentiation process was brought forward after DEN treatment. Interestingly, it is mentioned in the original description of the Solt-

[1]First Department of Pathology and Experimental Cancer Research, Semmelweis University, Budapest, Hungary.
[2]Department of Anatomy and Embriology, University of Medicine and Pharmacy Targu Mures, Targu Mures, Romania.
[3]Tumor Progression Research Group, Joint Research Organization of the Hungarian Academy of Sciences and Semmelweis University, Budapest, Hungary.

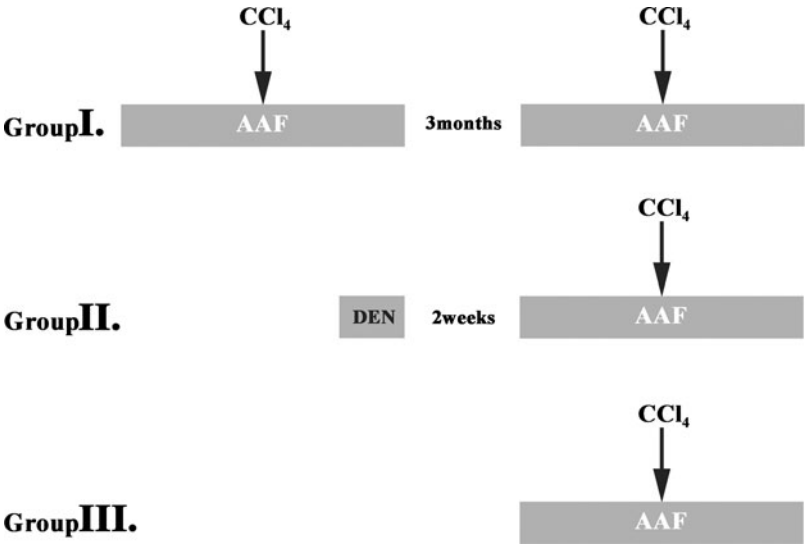

FIG. 1. Schematic representation of the injury models. Group **I**, 2×AAF/CCl_4; Group **II**, DEN-AAF/CCl_4; Group **III**, AAF/CCl_4.

Farber model that "oval cells" were present in the periportal zone after the DEN induced necrosis [9] (before the AAF administration). No further attention was paid to these ductules in the original report. They have not been characterized but their short description is reminiscent to the parenchymal ductules we have seen 3 months after the AAF/Ph experiment. These observations led us to analyze if (i) parenchymal ductules are present in the rat liver after different injuries, (ii) there is any similarity between the parenchymal ductules and canals of Hering, (iii) the presence of the parenchymal ductules have any impact on the regeneration induced by a repeated injury. Since the oval cell reaction in the AAF/Ph and AAF/CCl_4 experiments have been shown comparable [10,11] and our experimental design required repeated extensive parenchymal injuries on the same animal, surgical partial hepatectomy has been replaced by "chemical partial hepatectomy" with the application of a necrogenic dose of CCl_4.

Materials and Methods

Animal experiments

Male F344 rats were used for all experiments and were kept under standard conditions. At least four animals were used for each experimental time points. The animal study protocols were conducted according to National Institutes of Health guidelines for animal care.

Liver injury models. Traditional 2/3 surgical partial hepatectomy was performed [12].

Carbon tetrachloride: 2 mL/kg (20% CCl_4 dissolved in sunflower oil) was given by gavage.

Allyl alcohol: 50 μL/kg (diluted 1:40 in saline) was injected intraperitoneally.

DEN 200 mg/kg was injected intraperitoneally. Livers were removed 14 days and 12 weeks after DEN administration.

AAF/CCl_4 experiment: 8 mg/kg AAF was given by gavage for 5 days. CCl_4 treatment was given the next day as described above and it was followed by five more doses of AAF daily. Livers were removed 12 weeks after CCL_4 administration.

Repeated injury models. On the first group (2×AAF/CCl_4), AAF/CCl_4 experiment was performed and 3 months after the first CCl4 treatment the very same experiment was repeated (Group I).

The second group (DEN-AAF/CCl_4) was treated by a single dose of DEN and 2 weeks later the AAF/CCl_4 experiment was performed (Group II).

The control group (AAF/CCl_4, Group III) was stomach tubed with the solvent only (parallel to Group I), saline was injected into their peritoneal cavity together with the DEN treatment of Group II and finally the AAF/CCl_4 experiment was performed. In other words, AAF/CCl_4 experiment was performed on three sets of rats but it was preceded by another AAF/CCl_4 experiment 3 months earlier (Group I) or by DEN treatment 2 weeks earlier (Group II) or no pretreatment (Group III) (Fig. 1). The animals in each test

Table 1. Primary Antibodies and Fluorescent Dyes Used for the Immunohistochemical Studies

Antibody	*Species*	*Manufacturer*	*Catalog number*	*Dilution*
FITC-labeled pancytokeratin (CK5,6,8,17 and 19)	Mouse monoclonal	DAKO	F0859	1:10
CK7	Mouse monoclonal	Biogenex	NU255UC	1:50
CK19	Mouse monoclonal	Novocastra	NCL-CK19	1:50
AFP	Rabbit polyclonal	DAKO	A0008	1:100
DLK-1	Goat polyclonal	R&D Systems	AF1144	1:50
Laminin	Rabbit polyclonal	DAKO	Z0097	1:200
SMA	Mouse monoclonal	DAKO	M0851	1:50
OV-6	Mouse monoclonal	R&D Systems	MAB2020	1:100
TRITC-labeled streptavidin	—	Jackson Immunoresearch	016-090-084	1:100

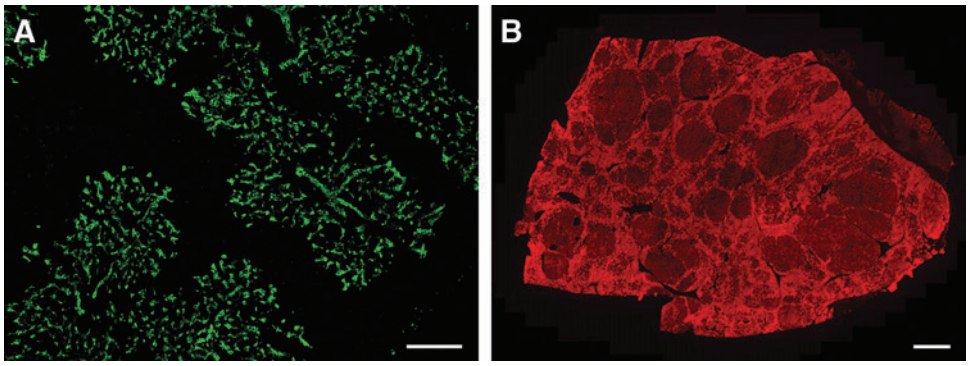

FIG. 2. **(A)** Representative image used to determine the area fraction of the OV6 positive ductules. **(B)** Scanned image of a whole liver section stained for endogen biotin by streptavidin TRITC. The foci appearing as dark areas as the new hepatocytes have low biotin content. Number and size of the foci were determined along with the area of the section to calculate the volume density of the foci. Scale bar for **(A)** 200 μm; **(B)** 1 mm.

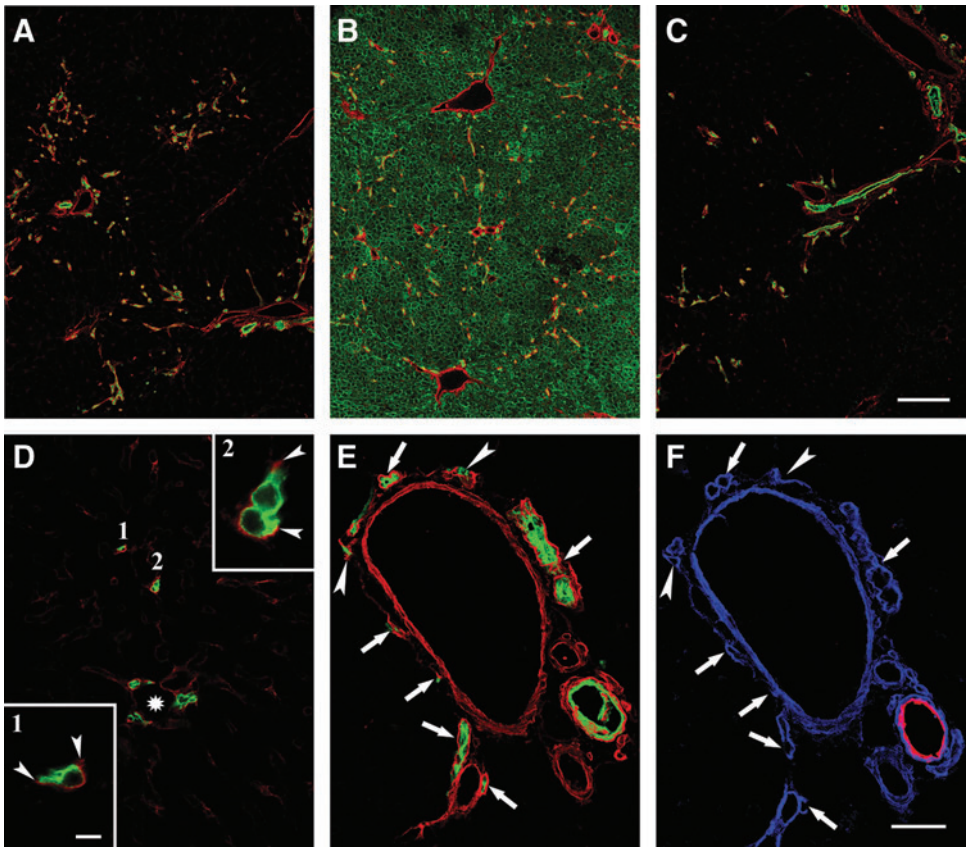

FIG. 3. **(A)** Liver cryosection 12 weeks after the AAF/CCl_4 experiment stained for OV6 (*green*) and laminin (*red*). Note the presence of scattered OV6 positive ductules apart from the portal tracts within the parenchyma. **(B)** Liver cryosection 14 days after DEN treatment stained for pan cytokeratin (*green*) and laminin (*red*). Numerous strong cytokeratin positive ductules surrounded by laminin positive basement membrane are present in the parenchyma. **(C)** Liver cryosection 12 weeks after DEN treatment stained for OV6 (*green*) and laminin (*red*). Scattered OV6 positive ductules are present in the parenchyma. **(D)** Liver cryosection 14 days after DEN treatment stained for OV6 (*green*) and laminin (*red*). Two parenchymal ductules are visible (1,2), which are attached to hepatocytes. *Insets* show the U-shaped basement membrane bordering the terminal part of these parenchymal ductules. *Arrowheads* point at the position where the basement membrane touches the hepatocyte. *Asterisk* indicates portal vein. Scale bar for the *insets:* 10 μm. **(E, F)** Serial cryosections of a normal liver depicting a portal area. **(E)** is stained for CK19 (*green*) and laminin (*red*). **(F)** is stained for CK7 (*red*) and laminin (*blue*). *Arrows* point at small ductules, which are negative for CK7. *Arrowheads* points at the same type of ductules, which are surrounded by an U shaped basement membrane. Note the large bile duct positive for both cytokeratins. Scale bar for **(A–C)** 200 μm; **(D–F)** 50 μm. CK, cytokeratin.

groups were the same age (5 months) and had similar weight when the AAF/CCl_4 treatment was started. The rats in different groups were sacrificed in identical time points. The intensity of the regeneration (oval cell proliferation/differentiation) was quantitatively characterized by measuring the area occupied by OV6 positive oval cells and determining the number of foci constructed by low biotin containing new hepatocytes.

Carcinogenesis experiments. The above described experiments were performed on additional animals. After completing the three sets of treatments, the rats were maintained on regular conditions and sacrificed at 15 months age. Thorough autopsy was performed and tumor suspicious lesions from the liver were fixed in formaldehyde for histological examination.

Immunohistochemistry

Frozen sections (15 μm) were fixed in methanol (−20°C) and were incubated at room temperature (1 h) with a mixture of the primary antibodies (Table 1), and then with appropriate secondary antibodies (Jackson ImmunoResearch). All samples were analyzed by confocal laser scanning microscopy using the Bio-Rad MRC-1024 system (Bio-Rad).

Morphometry

Determination of the area fraction occupied by OV6 positive ductules. Sections stained for OV6 were captured by a Bio-Rad confocal microscope using a 10× objective (Fig. 2A). The micrographs were transformed into black and white and the area occupied by OV6 positive oval cells was measured using the IMAN 2.0 program (KFKI). Livers from three to four animals were analyzed at each time-point.

Determination of volume density of foci. Sections were incubated with streptavidin-TRITC to highlight the endogen biotin of the hepatocytes and were scanned using the Mirax scanner (3DHISTECH). Small hepatocytes forming foci, due to their low endogen biotin content, appear as dark circles on the sections (Fig. 2B). The area of the section (A), the number (N) and diameter (d) of the foci were determined by the Mirax Viewer 1.11 program (3DHISTECH). Numerical density (Na = N/A) of the foci was calculated for each section. The real average diameter of the foci was calculated using the following formula: $D = (4/\prod) \times d$. Volume density of the foci was calculated by the following equation: Nv = Na/D. Livers from three to four animals were analyzed at each time-point.

Results

Parenchymal ductules can be induced by AAF/CCl_4 experiment and DEN administration

We have described the presence of CK7−/19+ ductules in the liver parenchyma 3 months after the completion of the AAF/Ph experiment [5]. The partial hepatectomy of this model can be replaced by a single, large dose CCl_4 poisoning (chemical hepatectomy). The AAF/CCl_4 experimental model is comparable to the original AAF/Ph experiment [10,11]. Confirming our results on the AAF/Ph model [5], parenchymal ductules could be observed in the liver of rats 3 months after the completion of the AAF/CCl_4 model (Fig. 3A). To investigate if parenchymal ductules can be induced by other forms of liver damage, more experimental models were checked. Surgical partial hepatectomy and CCl_4 poisoning themselves or allyl alcohol treatment resulted in no such ductules (data not shown). However, a single large dose of DEN (200 mg/kg) resulted in liver necrosis, and morphologically similar parenchymal ductules in the same distribution appeared in the liver upon the disappearance of necrosis (Fig. 3B) and were present up to 3 months during our observation period (Fig. 3C). They ended up on a hepatocyte, surrounded by open U-shaped basement membrane (Fig. 3D) as the canals of Hering (Fig. 3E, F) [4].

Characterization of parenchymal ductules (Table 2)

Ductular reactions are quite common in the liver, and the phenotype of the ductules is rather variable [13]. Although no reproducible classification of the ductular reactions exists, certain features are highly characteristic for certain types of ductules. The canals of Hering in normal, resting rat liver are characterized by a unique CK7−/19+ cytokeratin phenotype (Fig. 3E, F). The parenchymal ductules also do not express CK7 (Fig. 4A, B), while the activated oval cells do (Fig. 4C) [5]. There are no SMA expressing myofibroblasts around the canals of Hering and parenchymal ductules (Fig. 4D, E), but they are closely associated with the activated oval cells (Fig. 4F). Alpha-fetoprotein (AFP) (data not shown) and delta-like protein (DLK) are also not expressed by the canals of Hering and the parenchymal ductules (Fig. 4G, H) but are distinctive markers of the oval cells in rat liver (Fig. 4I) [14,15]. In fact, all the described features of the parenchymal ductules, except their distribution are consistent with the resting canals of Hering and are different from their activated progenies the so called oval cells [5].

Oval cell proliferation/differentiation is advanced in livers with parenchymal ductules

The canals of Hering are regarded as the niche of hepatic stem cells [4,15]. We were curious if the presence of the intraparenchymal ductules, which had a phenotype similar to the canals of Hering had any impact on the oval cell proliferation/differentiation triggered by the AAF/CCl_4 protocol. This experiment was performed on three different groups of rats. The intensity and dynamics of oval cell proliferation was characterized by the morphometric determination of the area covered by the "oval cell specific" OV6 antibody (Fig. 5). To quantitate the hepatocytic differentiation, the number of

Table 2. Immunophenotype of the Ductules

	Canals of hering	Intraparenchymal ductules		Oval cells
		DEN[a]	AAF/CCL_4[b]	
OV-6	+	+	+	+
CK19	+	+	+	+
CK7	−	−	−	+
SMA	−	−	−	+
DLK-1	−	−	−	+

[a]14 days and 12 weeks after DEN administration.
[b]12 weeks after AAF/CCL_4 experiment.

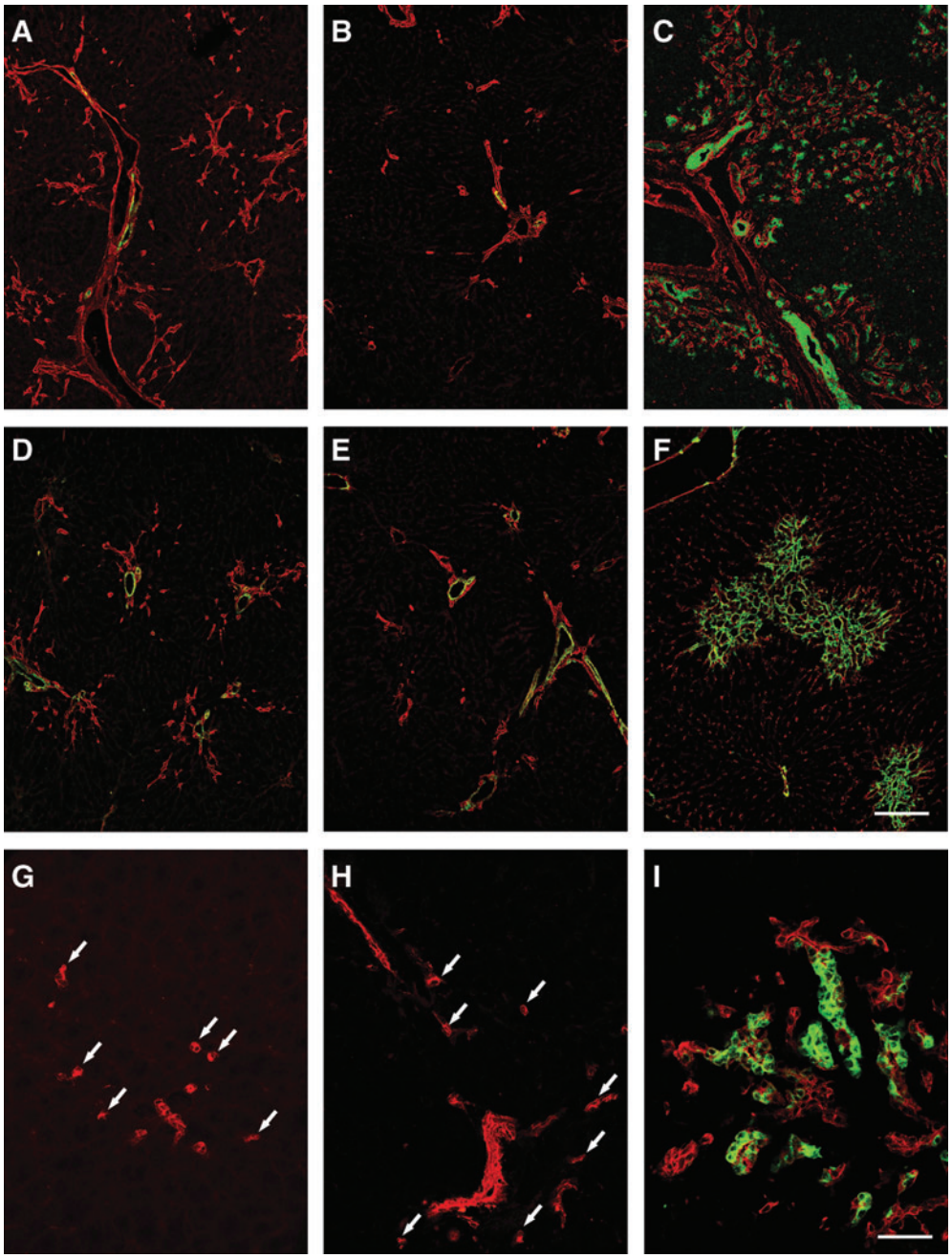

FIG. 4. Characterization of ductules present in the liver parenchyma 12 weeks after AAF/CCL_4 **(A, D, G)**, DEN **(B, E, H)** injury and 8 days after PH in the AAF/PH model **(C, F, I)**. **(A)** Liver cryosection after the AAF/CCl_4 experiment stained for CK7 (*green*) and laminin (*red*). The scattered parenchymal ductules surrounded by laminin are negative for CK7. In contrast CK7 positive bile ducts are present in the portal tracts. **(B)** Liver cryosection 12 weeks after DEN treatment stained for CK7 (*green*) and laminin (*red*). The parenchymal ductules are negative for CK7. **(C)** Liver cryosection 8 days after PH (AAF/PH experiment). The oval cell ductules spreading into the parenchyma are positive for CK7 (*green*) (*red*; laminin). SMA positivity (*green*) is confined only to vessels of the portal and central areas 12 weeks after AAF/CCL_4, **(D)** and DEN **(E)** injury. The parenchymal ductules are not surrounded by SMA positive cells (*red*; laminin). These ductules (*arrows*) also lack DLK expression **(G, H)** (*red*; OV-6). In contrast oval cell ductules are surrounded by a large amount of SMA positive cells (*green*) **(F)** and a portion of them is positive for DLK (*green*) **(I)**. Scale bar for **(A–F)** 200 μm; **(G–I)** 50 μm. AAF/Ph, 2-acetaminofluorene/partial hepatectomy.

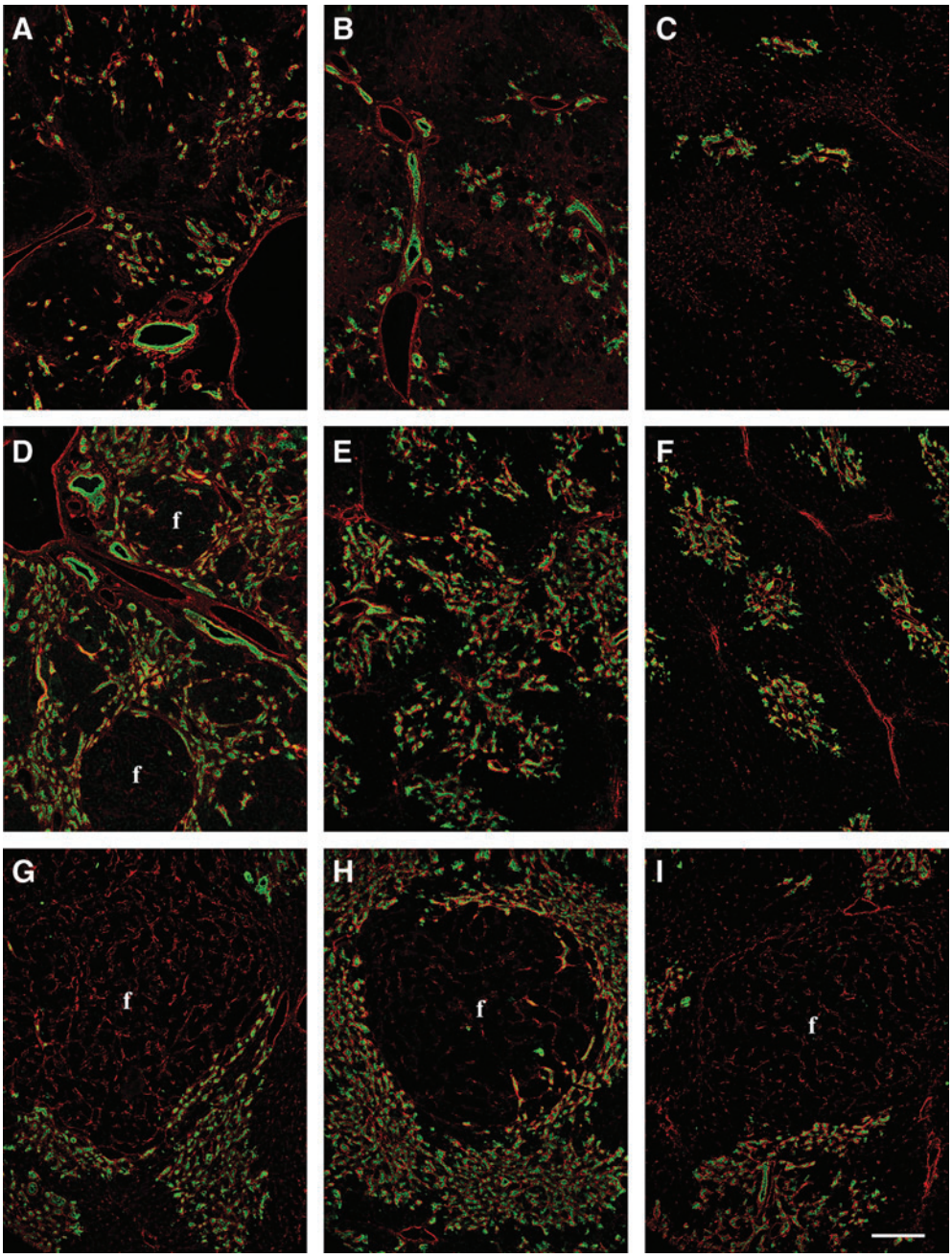

FIG. 5. Representative images of the dynamics of the expansion of oval cells and appearance and growth of foci. The three columns of micrographs correspond to the three models used. DEN-AAF/CCl_4, (Group II) **(A, D, G),** 2, 6, 10 days after chemical hepatectomy, respectively; 2×AAF/CCl_4, (Group I) **(B, E, H),** 2, 6, 10 days after chemical hepatectomy, respectively; AAF/CCl_4, (Group III) **(C, F, I),** 2, 6, 10 days after chemical hepatectomy, respectively. (f, foci, *green*; OV6, *red*; laminin). Scale bar for **(A–I)** 200 μm.

"small hepatocyte" foci was counted in the livers of experimental animals. While the peak of oval cell proliferation was on days 6 in Groups I and II, (groups with parenchymal ductules) the highest value was reached on day 12 in the control (III) group (Fig. 6A). The ductules induced by the AAF/CCl_4 experiment (the second one in group I) showed all the features of typical oval cell ducts, for example, they became CK7 and DLK positive and were surrounded by a large amount of SMA positive cells (Fig. 7). Similarly, while foci appeared on day 4 after chemical hepatectomy in the pretreated animals (groups I and II with parenchymal ductules), they were first seen only on day 10 in controls (Group III) (Fig. 6B). That is the livers with parenchymal ductules respond faster to the regenerative trigger.

Expansion of the stem cell compartment is not carcinogenic per se

Another set of animals from each group were saved for an additional 10 months and were sacrificed at 15 months age. The

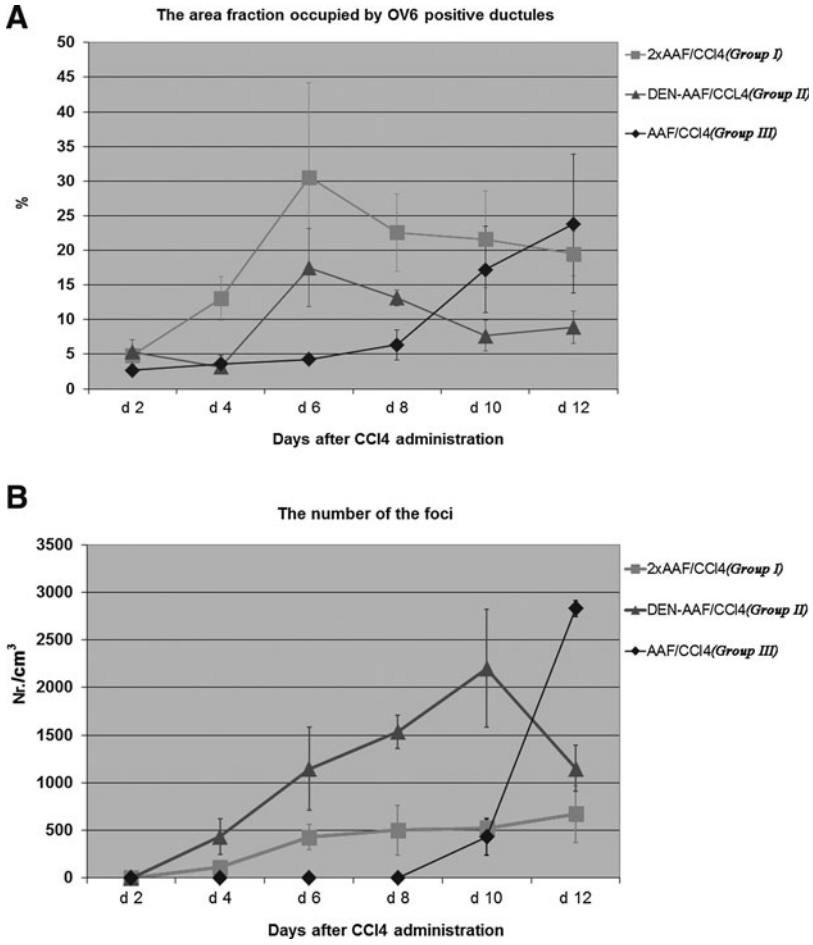

FIG. 6. **(A)** The dynamics of the expansion of oval cells in the different injury models 2, 6, 8 and 10 days after chemical hepatectomy (the bar represents SE). **(B)** The number of foci/cm^3 of liver in the different injury models 2, 6, 8 and 10 days after chemical hepatectomy (the bar represents SE).

livers were investigated for the presence of tumors or tumor precursor lesions. Histological examination of each nodular lesion was performed. The result is summarized in Table 3. The DEN-AAF/CCl_4 treatment proved to be an efficient hepatocarcinogenic protocol but one or two cycles of AAF/CCl_4 treatment resulted in only sporadic tumorous liver lesions.

Discussion

We have observed that, after certain manipulations, ductular structures are present in the rat liver parenchyma; we propose to call them parenchymal ductules. In addition, the stem cell mediated regeneration is faster in these livers.

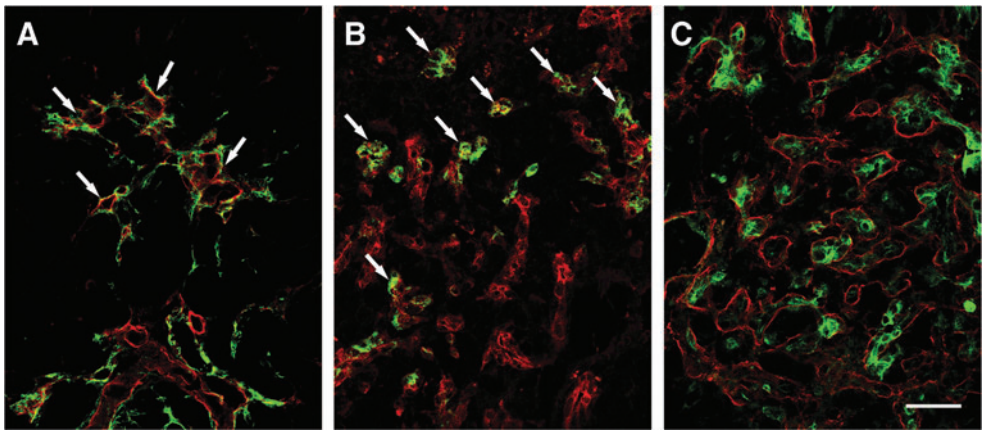

FIG. 7. Phenotypic characterization of the ductules present in the liver parenchyma in the three model systems after injury. **(A)** DEN-AAF/CCl_4 (Group II), 4 days after chemical hepatectomy, **(B)** 2×AAF/CCl_4 (Group I), 4 days after the second chemical hepatectomy, **(C).** AAF/CCl_4 (Group III), 10 days after the chemical hepatectomy. **(A)** The ductules present in the liver parenchyma are surrounded by SMA (*green*) positive cells (*arrows*) (*red*; laminin). **(B)** A portion of the ductules (*arrows*) are positive for DLK (*green*) (*red*; OV6). **(C)** All of the ductules are positive for CK7 (*green*) (*red*; laminin) Scale bar for **(A–C)** 50 μm.

Table 3. Tumorigenic Potential of the Different Experimental Protocols (12 Months After Beginning)

Experimental model	*Number of animals*	*Number and percentage of animals with nodules*	*Number and percentage of animals with carcinoma*
2×AAF/CCl_4 (Group I)	13	0 (0%)	1 (7.6%)
DEN-AAF/CCL_4 (Group II)	11	1 (9%)	8 (72.7%)
AAF/CCl_4 (Group III)	24	1 (4.1%)	0 (0%)

The existence of the hepatic stem cell compartment is mostly accepted, these cells and the hepatocytes play the major role in liver regeneration. There are several candidate cell populations for the stem cells [16] but most probably the canals of Hering constitute the niche for them [4,15]. We have analyzed these canals in detail and described that in rat liver they: (i) are strictly confined to the periportal connective tissue [5] (ii) are characterized by a unique CK7−/19+ cytokeratin phenotype. The activated progenies of canals of Hering, the so-called oval cells, (i) spread into the parenchyma, (ii) become CK7 positive, and (iii) start to express several marker proteins, for example, AFP and DLK [14,15] (iv) and are surrounded by SMA positive myofibroblasts. Ductular reactions are quite common in hepatic tissue [13,17]. These are morphologically rather heterogenous reactions probably with different etiologies and biological functions. Their exact role is still debated, and there is no generally accepted terminology or classification for them. We can observe parenchymal ductules 2 weeks after the administration of a necrogenic dose of DEN and 3 months after the AAF/CCl_4 experiments in otherwise mostly normal hepatic tissue. These are quite narrow tubules reminiscent of the canals of Hering, except for their spatial distribution. Their immunophenotype is also identical: they are (i) CK7−/19+, (ii) do not express AFP and DLK, (iii) are not enwrapped with SMA positive myofibroblasts. In addition their terminal tip ends up on a hepatocyte surrounded by an open U shaped basement membrane. Based on these features, they might correspond to hepatic stem cells.

It is reproducibly documented that the stem cells can participate in liver regeneration when the proliferation of hepatocytes is suppressed. [18,19]. The AAF/Ph or AAF/CCl_4 are among the most often used experimental models for stem cell mediated liver regeneration. Ductular proliferation was reported after DEN administration in rat and monkey liver as well [9,20], while the stem cell compartment is not or hardly activated after partial hepatectomy, CCl_4 poisoning or allyl alcohol treatment [18]. Our results suggest that, upon the completion of progenitor cell mediated regeneration, when the majority of the oval cells differentiate into hepatocytes or disappear by apoptosis, some of them reverse into the phenotype of resting canals of Hering. However, different from the original ones, they reside outside the periportal connective tissue in the lobules. The presence of these structures in the liver can be considered as the expansion of the stem cell compartment. Expansion of hepatic progenitor cell compartment has been reported in rats after portal branch ligation [21]. In human liver, severe parenchymal damages like steatosis [22] or HBV infection [23] resulted in similar reactions. TGF beta has been reported to participate in the regulation of this reaction and the expression of this multifunctional growth factor is increased in these experimental models [24]. Expansion of stem/progenitor cell pool has been observed in other tissues as well [25]. While the expansion of hematopoietic stem cells promoted multilineage hematopoiesis [26], age-related decline of progenitor cells reduced the regenerative capacity of kidney [27] and liver [28]. We compared the AAF/CCl_4 induced regeneration of unchallenged livers and livers with parenchymal ductules. Both oval cell expansion and the formation of hepatocytic foci happened significantly earlier in the livers with parenchymal ductules, supporting the idea that the presence of parenchymal ductules represents really expanded stem cell compartment. This result opens a new theoretical option for increasing the endogenous regenerative capacity of the liver. The amplification of stem/progenitor cell pool carries increased risk of tumor formation [29–35], although there are contradictory results as well [36]. Our results show that the DEN-AAF/CCl_4 model is as efficient a carcinogenesis model as the original Solt-Farber model and that the AAF/CCl_4 treatment is a powerful tumor promoter. However, the 2×AAF/CCl_4 treated rats did not have significantly more tumors than the controls. Thus, the increased number of stem cells does not indicate persistently higher tumor incidence. The recently revealed new results about the regulation of the stem cell compartment [31–36] may give us the tool to safely expand the pool of these cells in liver, which may result in clinically applicable increased regenerative capacity.

Finally, the presence of parenchymal ductules can represent an imprint of an earlier liver damage. Interestingly, multigenerational epigenetic adaptation of the hepatic fibrotic response has been reported [37] recently. The progenitor cell mediated accelerated liver regeneration in response to repeated challenges may also indicate a similar adaptation. Its transgenerational nature and molecular mechanism will, however, require further studies.

Acknowledgments

The authors would like to thank Renáta Kiss for her technical assistance.

Financial support: supported by Hungarian Scientific Research Fund (OTKA K100931 and PD109201)

Author Disclosure Statement

No competing financial interests exist.

References

1. Russo FP and M Parola. (2012). Stem cells in liver failure. Best Pract Res Clin Gastroenterol 26:35–45.
2. Katoonizadeh A, F Nevens, C Verslype, J Pirenne and T Roskams. (2006). Liver regeneration in acute severe liver impairment: a clinicopathological correlation study. Liver Int 26:1225–1233.

3. Tetamatsu M, H Ho, T Kaku, JK Ekem and E Farber. (1984). Studies on the proliferation and fate of oval cells in the liver of rats treated with 2-acetylaminofluorene and partial hepatectomy. Am J Pathol 114:418–430.
4. Paku S, J Schnur, P Nagy and SS Thorgeirsson. (2001). Origin and structural evolution of the early proliferating oval cells in rat liver. Am J Pathol 158:1313–1323.
5. Paku S, K Dezső, L Kopper and P Nagy. (2005). Immunohistochemical analysis of cytokeratin 7 expression in resting and proliferating biliary structures of rat liver. Hepatology 42:863–870.
6. Evarts RP, P Nagy, E Marsden and SS Thorgeirsson. (1987). A precursor-product relationship exists between oval cells and hepatocytes in rat liver. Carcinogenesis 8:1737–1740.
7. Dezső K, V Papp, E Bugyik, H Hegyesi, G Sáfrány, CS Bödör, P, Nagy and S Paku. (2012). Structural analysis of oval-cell-mediated liver regeneration in rats. Hepatology 56:1457–1467.
8. Solt D and E Farber. (1976). New principle for the analysis of chemical carcinogenesis. Nature 263:701–703.
9. Solt DB, A Medline and E Farber. (1977). Rapid emergence of carcinogen-induced hyperplastic lesions in a new model for the sequential analysis of liver carcinogenesis. Am J Pathol 88:595–609.
10. Petersen BE, VF Zajac and GK Michalopoulos. (1998). Hepatic oval cell activation in response to injury following chemically induced periportal or pericentral damage in rats. Hepatology 27:1030–1038.
11. Chiu CC, GT Huang, SH Chou, CT Chien, LL Chiou, MH Chang, HS Lee and DS Chen. (2007). Characterization of cytokeratin 19 positive hepatocyte foci in the regenerative rat liver after 2-AAF/CCl_4 injury. Histochem Cell Biol 128:217–226.
12. Higgins GM and RM Anderson. (1931). Experimental pathology of the liver: restoration of the liver of the white rat following partial surgical removal. Exp Pathol 12:186–202.
13. Turányi E, K Dezső, J Csomor, Z Schaff, S Paku and P Nagy. (2010). Immunohistochemical classification of ductular reactions in human liver. Histopathology 57:607–614.
14. Jensen CH, EI Jauho, E Santoni-Rugiu, U Holmskov, B Teisner, N Tygstrup and HC Bisgaard. (2004). Transit amplifying ductular (oval) cells and their hepatocytic progeny are characterized by a novel and distinctive expression of delta like protein/preadipocyte factor1/fetal antigen 1. Am J Pathol 164:1347–1359.
15. Santoni-Rugiu E, P Jelnes, SS Thorgeirsson and HC Bisgaard. (2005). Progenitor cells in liver regeneration: molecular responses controlling their activation and expansion. APMIS 113:876–902.
16. Kuwahara R, AV Kofman, Ch S Landis, ES Swenson, E Barendswaard and ND Theise. (2008). The hepatic stem cell niche: identification by label-retaining cell assay. Hepatology 47:1994–2002.
17. Roskams TA, ND Theise, C Balabaud, G Bhagat, PS Bhatal, P Bioulac-Sage, EM Brunt, JM Crawford, HA Crosby, et al. (2004). Nomenclature of the finer branches of biliary tree: canals, ductules, and ductular reactions in human livers. Hepatology 39:1739–1745.
18. Malato Y, S Naqvi, N Schurmann, R Ng, B Wang, J Zape, et al. (2011). Fate tracing of mature hepatocytes in mouse liver homeostasis and regeneration. J Clin Invest 121:4851–4860.
19. Michalopoulos GK. (2010). Liver regeneration after partial hepatectomy: critical analysis of mechanistic dilemmas. Am J Pathol 176:2–13.
20. Lapis K, I Sarosi, J Bocsi and UP Thorgeisson. (1995). Cytokeratin patterns of liver carcinomas induced by diethylnitrosamine in monkeys. Lab Invest 72:748–759.
21. Sakai H, Y Tagawa, M Tamai, H Motoyama, S Ogawa, J Soeda, T Nakata and S Miyagawa. (2010). Isolation and characterization of portal branch ligation-stimulated Hmga2-positive bipotent hepatic progenitor cells. Biochem Biophys Res Com 403:298–304.
22. Cho JY, KS Suh, WY Shin, HW Lee, NJ Yi, MA Kim, JJ Jang and KU Lee. (2010). Expansion of hepatic progenitor cell in fatty liver graft after living donor liver transplantation. Transpl Int 23:530–537.
23. Wu N, F Liu, H Ma, FX Zhu, ZD Liu, R Fei, HS Chen, H Wang and L Wei. (2009). HBV infection involving in hepatic progenitor cells expansion in HBV-infected end-stage liver disease. Hepatogastroenterology 56:964–967.
24. Thenappan A, Y Li, K Kitisin, A Rashid, K Shetty, L Johnson and L Mishra. (2010). Role of Transforming growth factor β signaling and expansion of progenitor cells in regenerating liver. Hepatology 51:1373–1382.
25. Johnnidis JB, MH Harris, RT Wheeler, S Stehling-Sun, MH Lam, O Kirak, TR Brummelkamp, MD Fleming and FD Camargo. (2008). Regulation of progenitor cell proliferation and granulocyte function by microRNA-223. Nature 451: 1125–1129.
26. Sun H, I Nowak, J Liesveld and Y Chen. (2012). Eltrombopag, a thrombopoietin receptor agonist, enhances human umbilical cord blood hematopoetic stem/primitive progenitor cell expansion and promotes multi-lineage hematopoesis. Stem Cell Res 9:77–86.
27. Miya M, A Maeshima, K Mishima, N Sarurai, H Ikeuchi, T Kuroiwa, K Hiromura and Y Nojima. (2012). Age-related decline in label-retaining tubular cells: implication for reduced regenerative capacity after injury in the aging kidney. Am J Physiol Renal Physiol 302:F694-F702.
28. Ono Y, S Kawachi, T Hayashida, M Wakui, M Tanabe, O Itano, H Obara, M Shinoda, T Hibi, et al. (2011). The influence of donor age on liver regeneration and hepatic progenitor cell populations. Surgery 150:154–161.
29. Popova NV, KA Teti, KQ Wu and RJ Morris. (2003). Identification of two keratinocyte stem cell regulatory loci implicated in skin carcinogenesis. Carcinogenesis 24: 417–425.
30. Yang W, HX Yan, L Chen, Q Liu, YQ He, LX Yu, SH Zhang, DD Huang, L Tang, et al. (2008). Wnt/beta-catenin signaling contributes to activation of normal and tumorigenic liver progenitor cells. Cancer Res 68:4287–4295.
31. Joshi PA, HW Jackson, AG Beristain, MA Di Grappa, PA Mote, CL Clarke, J Stingl, PD Waterhouse and R Khokha. (2010). Progesterone induces adult mammary stem cell expansion. Nature 465:803–807.
32. Gemenetzidis E, D Elena-Costea, EK Parkinson, A Waseem, H Wan and MT Teh. (2010). Induction of human epithelial stem/progenitor expansion by FOXM1. Cancer Res 70:9515–9526.
33. Li Y, LM Vecchiarelli-Federioco, YJ Li, SE Egan, D Spaner, MR Hough and Y Ben-David. (2012). The miR-17–92 cluster expands multipotent hematopoetic progenitors whereas imbalanced expression of its individual oncogenic miRNAs promotes leukemia in mice. Blood 119:4486–4498.
34. Benhamouche S, M Curto, I Saotome, AB Gladden, C Liu, M Giovannini and AI McClatchey. (2010). Nf2/Merlin controls progenitor homeostasis and tumorigenesis in the liver. Genes Dev 24:1718–1730.

35. Wang AY, S Yeh, T Tsai, H Huang, Y Jeng, W Lin, W Chen, K Yeh, P Chen and D Chen. (2011). Depletion of β-catenins from mature hepatocytes of mice promotes expansion of hepatic progenitor cells and tumor development. PNAS 108:18384–18389.
36. Nieuwenhuis E, PC Barnfield, S Makino and CC Hui. (2007). Epidermal hyperplasia and expansion of the interfollicuar stem cell compartment in mutant mice with a C-terinal truncation of Patched1. Dev Biol 308:547–560.
37. Zeybel M, T Hardy, YK Wong, JC Mathers, CR Fox, A Gackowska, F Oakley, AD Burt, CI Wilson, et al. (2012). Multigenerational epigenetic adaptation of the hepatic wound-healing response. Nat Med 18.1369–1379.

Address correspondence to:
Dr. Péter Nagy
First Department of Pathology and Experimental Cancer Research
Semmelweis University
Budapest Üllõi út 26
H-1085
Hungary

E-mail: nagy@korb1.sote.hu

Received for publication April 30, 2013
Accepted after revision August 14, 2013
Prepublished on Liebert Instant Online August 17, 2013